Pergamon

Cement and Concrete Research 33 (2003) 305–316

CEMENT AND CONCRETE RESEARCH

Cementation of a low-level radioactive waste of complex chemistry Investigation of the combined action of borate, chloride, sulfate and phosphate on cement hydration using response surface methodology

C. Cau Dit Coumes[a,*], S. Courtois[b]

[a]*Commissariat à l'Energie Atomique, DED/SEP/LCC, Bât. 332, CEN Cadarache, 13108 Saint-Paul-Lez-Durance cedex, France*
[b]*EAMS², Université Aix-Marseille II, IUT GMP, avenue Gaston Berger, 13625 Aix-en-Provence cedex 1, France*

Received 18 February 2002; accepted 24 July 2002

Abstract

A cement-based grout formulation was investigated to immobilize low-level radioactive evaporator concentrates with widely variable chemical composition. The objective was to determine the sensitivity of the solidified waste forms characteristics on a variation in the concentrations of four components of the waste (boron, chloride, sulfate and phosphate). Providing adequate changes of variables, the problem was shown to amount to a mixture study with constraints placed on each factor. Experimental design methodology enabled to build empirical models (special cubic models in the canonical form), which gave a satisfactory description of the responses (viscosity of the grout, heat of hydration of cement, compressive strength and expansion of $4 \times 4 \times 16$ cm specimens after 90 days of wet curing) within the region of the experimental data, and which could be used as prediction tools. High contents of phosphate in the waste (>25 $g \cdot l^{-1}$) were shown to improve most properties of the elaborated materials. In particular, setting time, rate of heat production and swelling under water were decreased, while grout workability was enhanced.

Keywords: Waste management; Setting; Workability; Expansion; Mechanical properties

1. Introduction

Cementation is a widely applied technique for the conditioning of low- and intermediate-level radioactive wastes [1]. In particular, the use of cement to immobilize evaporator concentrates from aqueous effluents treatment is an attractive procedure. Hydrated products may be formed by the participation of some of the waste chemical species in the hydration process; some species may be adsorbed on the several hydrated compounds formed, and a significant amount of liquid containing soluble salts can be restrained and rendered somewhat immobile in the highly tortuous porous network formed in the hardened grout. Although the chemical and physical properties of cement are well known and experience in using it for construction extends over many decades, knowledge of the effect of mixing cement with concentrates of complex chemistry is still limited and experimental work remains necessary to elaborate cement-waste formulations. It generally includes the three following steps: (i) setting of a proper formulation with an average synthetic waste, (ii) study of the flexibility of this formulation with synthetic wastes of variable chemistry, and (iii) final validation with real radioactive wastes. Step (ii) is essential since the quality of the final cemented waste forms often depends very much on the composition of the waste. With a classical experimental approach (for example, a one-variable-at-a-time strategy), the required number of trials in this phase may increase very rapidly, as soon as the concentrate contains several chemical species with widely variable concentrations. This article illustrates another approach, based on response surface methodology [2], which enables to keep the total number of trials within reason without compromising the quality of the achieved results.

2. Problem definition

Because arising from various research activities, the evaporator concentrate considered in this study is charac-

* Corresponding author. Tel.: +33-4-42-25-45-03; fax: +33-4-42-25-27-12.
E-mail address: cau-dit-coumes@desdsud.cea.fr (C. Cau Dit Coumes).

0008-8846/02/$ – see front matter © 2002 Elsevier Science Ltd. All rights reserved.
PII: S0008-8846(02)00943-2

terized by highly variable chemical and radiological compositions (Table 1). Its salinity is fixed to 300 g l^{-1}. Four components, boron, chloride, sulfate and phosphate, are known to affect significantly the rate of hydration of cement and/or reduce the quality of the product.

Borate and phosphate are reported to be strong retarders of cement setting and hardening [3–8]. Retardation may arise either from surface adsorption or from the formation of protective layers over the cement grains due to precipitation with calcium [9]. According to Roux [10], the borate inhibition effect might thus result from the formation of amorphous $2CaO{\cdot}3B_2O_3{\cdot}8H_2O$ from polyboric anions $B_3O_3(OH)_4^-$ and/or $B_3O_3(OH)_5^{2-}$. The exact mechanism of inhibition by phosphate is still an open question.

Chloride is on the contrary a strong accelerator of the early stages of cement hydration [11–13]. In hardened cement pastes, although much remains in the pore solution, some chloride is partly bound in poorly soluble Friedel's salt $C_3A{\cdot}CaCl_2{\cdot}10H_2O$ [14–18]. There is additional evidence suggesting that hydration products of C_4AF also take part in chloride binding [19, 20]. Furthermore, the high specific area of the amorphous C–S–H gel may substantially contribute to chloride binding through physical adsorption [21]. The chloride retention capacity can be affected by the presence of alkalis and sulfate during cement hydration because of the preferential reaction between sulfate and C_3A, and the competition for binding by cement hydrates between hydroxyl and chloride ions in the pore solution [22, 23]. With very concentrated chloride solutions (>>10 g l^{-1}), destructive oxychlorides ($3CaO{\cdot}CaCl_2{\cdot}15H_2O$, $CaO{\cdot}CaCl_2{\cdot}2H_2O$) may be formed.

As for sulfate, it retards C_3A and C_4AF hydration at low concentration ($\approx$1 g l^{-1}), which enables setting control [24]. At higher concentration (>10 g l^{-1}), false set may occur due to the interlocking of precipitated gypsum and ettringite crystals. There is an additional risk of expansion and cracking of the hardened paste due to topochemical formation of ettringite and gypsum with directional crystal growth, and swelling of colloidal ettringite by water absorption [25–28]. Damage may also result from decalcification of the C–S–H matrix, which leads to softening and disintegration, as reported for materials made with slag cements [29] or sulfate resistant Portland cements [30] in the case of external sulfate attack. Li et al. [31] described the deleterious formation of a mineral called "U" phase (a sodium substituted AFm phase) which occurred in the cemented low-level wastes containing high amounts of Na_2SO_4 (10–12%) and which induced a large expansion. This phase can form only at very high alkaline concentration, and transforms into ettringite when the alkalinity of the pore solution is decreased.

Table 1
Composition of the evaporator concentrate

Chemical	
Anions	Cations
NO_3^-: 160 g l^{-1}	NH_4^+: 0.1–11 g l^{-1}
B: 0–3 g l^{-1}	Na^+: variable concentration to maintain electroneutrality
Cl^-: 1–20 g l^{-1}	
SO_4^{2-}: 0.8–27 g l^{-1}	
PO_4^{3-}: 1–50 g l^{-1}	
Salinity of 300 g· l^{-1}	
Radiological	
^3H, ^{14}C, ^{54}Mn, ^{58}Co, ^{60}Co, ^{63}Ni, ^{65}Zn, ^{90}Sr, ^{110m}Ag, ^{124}Sb, ^{134}Cs, ^{135}Cs, ^{154}Eu, ^{238}Pu, ^{241}Am, etc.	
$\alpha < 16$ GBq m^{-3}/$\beta\gamma < 200$ GBq m^{-3}	

Table 2
Solidification process

Pretreatment (for 1-l waste)	Cementation (for 1-l grout)
Objectives:	
–Insolubilisation of strontium and cesium	
–Stripping of ammonia	
Heating of the waste at 60 °C	Pretreated waste 500 ml
Addition of 13.44 g of $Ba(OH)_2{\cdot}8H_2O$[a]	Plasticizer 5.5 g
Stirring at 60 °C for 15 min	Portland cement 1000 g
Addition of 3.7 g of $Ca_2Fe(CN)_6{\cdot}11H_2O$	Silica fume 100 g
Stirring at 60 °C for 60 min	Siliceous sand 374 g
Addition of sodium hydroxide (16 mol l^{-1}) until pH 11.7	
Stirring at 60 °C for 60 min	

[a] In the presence of sulfate and phosphate, barium hydroxide is converted into barium sulfate or phosphate, which results in a small decrease (<4 g l^{-1}) in the concentrations of these two ions in the liquid phase of the pretreated waste.

It should be noted that most available data are relative to each species taken separately from the others. Under the conditions of this study, additional complexity might be expected due to possible synergetic or antagonistic interactions between the species in mixture.

A two-stage process, including a chemical treatment prior to immobilization in cement, was first designed on the basis of a waste of average composition (Table 2). The objective was then to determine the sensitivity of the solidified waste form characteristics on a variation in the concentrations of boron, chloride, sulfate and phosphate in the waste.

3. Experimental design construction

The experimental design construction was based on the following procedure:

(i) selection of the variables (or factors) and experimental region of interest given the objectives of the study,
(ii) selection of the responses to characterize the phenomenon under investigation,
(iii) assumption of an *empirical* model for the responses,
(iv) and selection of a design that provides good estimates of the parameters in the model.

3.1. Factors and experimental domain

The factors were the boron, chloride, sulfate and phosphate concentrations in the evaporator concentrate prior to chemical treatment. The nitrate and ammonia concentrations were fixed respectively to 160 and 0.3 g l^{-1} in all runs. This latter value represented the residual concentration of ammonium after stripping, as measured industrially on real wastes. The experimental domain was defined by the expected ranges of variation of boron, chloride, sulfate and phosphate concentrations in the real waste (Table 1). It should be noticed that the factors could not vary independently from each other since the waste had a salinity of 300 g l^{-1} whatever its composition.

For the needs of the study, synthetic wastes were prepared by addition of ammonia and dissolution into water of boric acid and sodium salts of chloride, sulfate, phosphate and nitrate. Let X_1, X_2, X_3, X_4 and X_5 be the respective concentrations (in g l^{-1}) of boric acid, chloride, sulfate, phosphate and sodium brought in with these three anions. Given the constant concentration of nitrate, keeping the waste salinity to 300 g l^{-1} imposed:

$$X_1 + X_2 + X_3 + X_4 + X_5 = 80 \text{ g } l^{-1} \quad (\text{since } [NaNO_3] \approx 220 \text{ g } l^{-1}) \tag{1}$$

Eq. (2) was derived from electroneutrality of the added salts.

$$X_5 = 0.648X_2 + 0.479X_3 + 0.726X_4 \qquad (\text{in g } l^{-1}) \tag{2}$$

Introducing Eq. (2) into Eq. (1) led to:

$$X_1 + 1.648X_2 + 1.479X_3 + 1.726X_4 = 80 \qquad (\text{in g } l^{-1}) \tag{3}$$

or

$$X_1' + X_2' + X_3' + X_4' = 1 \tag{4}$$

with the new dimensionless variables:

$$X_1' = X_1/80 \quad X_2' = 1.648X_2/80$$
$$X_3' = 1.479X_3/80 \quad X_4' = 1.726X_4/80$$

Eq. (4) was characteristic of a four-component mixture problem, X_i' representing the proportion of component i in the total mixture [32,33]. X_i' could not vary from 0 to 1: it was constrained between a lower limit a_i and/or an upper limit b_i ($0 < a_i \le X_i' \le b_i < 1$), as shown in Table 3. The consistency of these constraints with Eq. (4) was checked by calculating:

- the component ranges $R_i = b_i - a_i$ (Table 3),
- the linear (as opposed to volumetric) measures of the size of simplex A and simplex B, the two regions respectively defined by the lower and upper bounds.

$$R_a = 1 - \sum_{i=1}^{4} a_1 = 0.942 \tag{5}$$

$$R_b = \sum_{i=1}^{4} b_1 - 1 = 1.127 \tag{6}$$

According to Crosier [34], any R_i greater than R_a indicates an inconsistent upper bound and any R_i greater than R_b an inconsistent lower bound. The comparison of the component ranges with R_a and R_b revealed an inconsistency: the upper bound for X_4' was unattainable since R_4 exceeded R_a. The upper constraint for X_4' was thus replaced by the implied limit defined as:

$$b_4^* = a_4 + R_a = 0.964 \tag{7}$$

and the value of R_b became 1.091.

The region of interest defined by these constraints resulted from the intersection of simplex A and simplex B. It has been shown [34] that any component range less than the smaller of R_a and R_b indicates that the experimental region is not a simplex. This was the case in this study since $R_p = \min(R_a, R_b)$ (0.942) exceeded R_1 (0.215), R_2 (0.391) and R_3 (0.485). The experimental domain was a convex polyhedron with 10 vertices (Fig. 1), as calculated with formula (8) of Crosier.

$$\text{Number of vertices} = q + \sum_{r=1}^{q} L(q,r)(q-2r) + \sum_{r=1}^{q} E(q,r)(1-r) \tag{8}$$

where q is the number of components, $L(q,r)$ the number of combinations of component ranges taken r at a time that sum to less than R_p and $E(q,r)$ the number of combinations of component ranges taken r at a time that sum to R_p.

3.2. Responses

Each elaborated material was evaluated for a number of properties including setting time, bleeding, fluidity after mixing, rise in temperature during hydration, compressive strength and dimensional stability. The desirable criteria were defined by taking into account both process requirements and near-surface disposal specifications (Table 4).

3.3. Postulated model

Response surface methodology is based on the hypothesis that the responses can be approximated, within the range of the data, by a low order polynomial model. The quadratic model has been found to give a reasonable fit to a large proportion of mixture response surfaces [33]. However, given the large region of interest and the usual

Table 3
Ranges of variation of normal and coded variables

Chemical	Normal variables		Coded variables				
				Explicit constraints	Range of variation R_i	Implicit constraints	Range of variation R_i
H_3BO_3	X_1	0–17.2 g l^{-1}	X_1'	$0 \le X_1' \le 0.215$	0.215	$0 \le X_1' \le 0.215$	0.215
Cl^-	X_2	1–20 g l^{-1}	X_2'	$0.021 \le X_2' \le 0.412$	0.391	$0.021 \le X_2' \le 0.412$	0.391
SO_4^{2-}	X_3	0.8–27 g l^{-1}	X_3'	$0.015 \le X_3' \le 0.5$	0.485	$0.015 \le X_3' \le 0.5$	0.485
PO_4^{3-}	X_4	1–50 g l^{-1}	X_4'	$0.022 \le X_4' \le 1$	0.978	$0.022 \le X_4' \le 0.964$	0.942
					$R_a = 0.942$		$R_a = 0.942$
					$R_b = 1.127$		$R_b = 1.091$

R_a and R_b are defined by Eqs. (5) and (6).

complexity of cementation studies, higher order terms were also included. The responses were thus assumed to be a function of the coded variables X_i' and the postulated model was a special cubic polynomial in the canonical form.

$$Y = \sum_{i=1}^{4} \beta_i X_i' + \sum_{1 \le i \le j}^{4} \beta_{ij} X_i' X_j' + \sum_{1 \le i < j < k}^{4} \beta_{ijk} X_i' X_j' X_k' + \varepsilon \quad (9)$$

where Y = experimental response and ε = random error.

This model, which should not be confused with interaction models for nonmixture variables, did not contain any constant term β_0, squared terms $X_i'^2$ or cubic terms $X_i'^3$. This simplification resulted from the fact that the levels of all components added to 1.

3.4. Experimental design

The positioning of experimental points within the experimental domain is of great importance to obtain a good precision on the estimates of the model parameters and, in a second step, on model-predicted response values. Let n be the number of design points and p the number of parameters in the model. The model can be written in matrix notation as:

$$\mathbf{Y} = \mathbf{XB} + \mathbf{e} \quad (10)$$

where $\mathbf{Y}$ is the $(n \times 1)$ vector of responses, $\mathbf{X}$ is the $(n \times p)$ matrix of model terms, $\mathbf{B}$ is the $(p \times 1)$ vector of unknown coefficients and $\mathbf{e}$ is the $(n \times 1)$ vector of errors with zero means and variance $\sigma^2\mathbf{I}$, σ^2 being the experimental error variance and $\mathbf{I}$ the $(n \times n)$ identity matrix. $\hat{\mathbf{B}}$, the least squares estimate of $\boldsymbol{B}$, is defined by:

$$\hat{\mathbf{B}} = (\mathbf{X}'\mathbf{X})^{-1}\mathbf{X}'\mathbf{Y} \quad (11)$$

It can be easily shown that the variance–covariance matrix for $\hat{\mathbf{B}}$ checks:

$$\text{Var}\ (\hat{\mathbf{B}}) = (\mathbf{X}'\mathbf{X})^{-1}\sigma^2 \quad (12)$$

and that the prediction variance at a point $\mathbf{x}$ is:

$$\text{Var}\ (\mathbf{x}) = d_x\sigma^2 \quad (13)$$

where $d_x = \mathbf{x}'(\mathbf{X}'\mathbf{X})^{-1}\mathbf{x}$ and $\mathbf{x}$ is a $(1 \times p)$ vector.

Relationships (12) and (13) are most important since they show how the experimental error affecting the response is

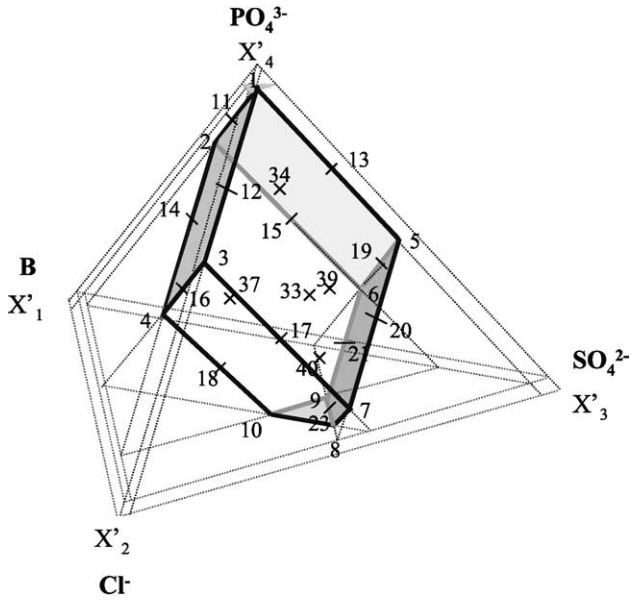

Fig. 1. Experimental domain and 27-point selected design.

Table 4
Criteria to assess the quality of encapsulated waste

Setting time	Final set should be higher than 5 h to avoid any setting in the mixer in case of technical hitch and lower than 24 h to enable good output of the conditioning unit.
Fluidity after mixing	Cemented waste should have a low viscosity after mixing in order to allow easy emptying of the drum and thus to minimize amounts of rinsing water.[a]
Bleeding	The material should not exhibit any bleeding after 24 h.
Rise in temperature in the grout during hydration	The rise in temperature resulting from cement hydration should not affect the package integrity.
Compressive strength	Compressive strength after 90 days of curing under water at 20 °C should exceed 8 MPa.
Dimensional stability	Any expansion, which may cause damage to the matrix or container, should be precluded.

[a] The envisaged process is in-line batch cementation.

transmitted to the estimates of the model coefficients and to the predicted response at point **x**. Two terms must be taken into account, the experimental error, which is not surprising, and matrix **X**, i.e., the distribution of the experimental points within the experimental domain and the analytical form of the model. As σ^2 is imposed by the environment, it is on matrix **X** that one should act to improve the model precision.

In order to estimate the 14 parameters of the model defined by Eq. (9), several designs were considered. The well-known simplex-lattice designs introduced by Scheffé [32,35] are useful when the proportions of all components in the mixture can vary from 0 to 1. Scheffé also discussed the use of pseudocomponents (components which are actually mixtures of two or more components) when some components are constrained. However, in order to use the simplex design in this situation, the ranges R_i of all the components have to be equal, which was not checked in the present study ($R_1 = 0.215$, $R_2 = 0.391$, $R_3 = 0.485$ and $R_4 = 0.942$). MacLean and Anderson [36] recommended the extreme vertices design for experimentation in constrained mixture spaces. This design was constructed from the 10 vertices, the 7 constraint plane centroids, the 15 edge centroids and the overall centroid of the previously defined polyhedron. Ten validation points corresponding to mixtures including all components and homogeneously distributed in the investigated domain were added for a total of 43 runs. This represented more trials than it was possible to run. A subset of this 43-point candidate list was therefore selected according to the following procedure. For n increasing from 14 (the number of trials should be at least equal to the number of coefficients in the model) to 35, the EXCHANGE algorithm [37] was used to define a n-point design which maximized $\det(\mathbf{X}'\mathbf{X})$, this parameter being inversely proportional to the generalized variance of the estimated coefficients. Additional statistical properties of that n-point design were evaluated: trace $(\mathbf{X}'\mathbf{X})^{-1}$, which was proportional to the average variance of the estimated coefficients, maximum prediction variance $d_{\max}$, which corresponded to the maximum value of d_X (see Eq. (13)) over the design points, and percent G efficiency $= 100 \cdot p/(n \cdot d_{\max})$. The 27-point design was selected because it represented a good compromise between the number of trials to run and the matrix performances. In particular, maximum prediction variance was lower than 1 ($d_{\max} = 0.88$) (i.e., the variance of the predicted response would be lower than that of the measured response provided that the model be correct) and G-efficiency exceeded 50%. Four replicates of the overall centroid were added in order to provide a measure of the experimental error, which led to a total of 31 runs.

4. Experimental

4.1. Preparation of synthetic wastes

Synthetic evaporator concentrates were prepared by dissolving boric acid and sodium salts (NaCl, Na_2SO_4, $NaNO_3$ and $Na_3PO_4 \cdot 12H_2O$ of analytical grade) in demineralized water and pretreated as described in Table 2. A small concentration of ammonia (0.3 g l^{-1}) was then added at ambient temperature in order to simulate the residual amount of NH_3 recorded in real wastes after stripping.

4.2. Reactants for waste encapsulation

The chemical and mineralogical composition of the sulfate-resistant Portland cement used in this study (CPA CEM I 52,5 PM ES CP2 from Lafarge) is detailed in Table 5. The formulation was optimized by adding non densified silica fume (Péchiney ND-LAU71) and siliceous sand with fine granulometry (< 350 μm) (Sifraco NE34). The grout workability was enhanced by using a superplasticizing admixture made of naphtalene sulfonate formaldehyde (Pozzolith 400N from MBT).

4.3. Protocols

Mixing was performed with a normalized (European standard EN 196-1) mortar mixer according to the following sequence: (1) introduction of pretreated waste and superplasticizer, (2) mixing at low speed, (3) addition of the premixed pulverulents (cement, sand and silica fume) while maintaining slow stirring and (4) mixing at low speed for 3 min.

Elaborated materials were characterized by measuring various parameters according to normalized procedures: bleeding (French standard NF P 18-359), heat of hydration (NF P 15-436), swelling (NF P 15-433) and compressive strength (EN 196-1) of parallelepipedic samples (4 × 4 × 16 cm) cured for 90 days at 20 °C under water. Viscosity of the grout after mixing was estimated by measuring the torque on a rotating blade at constant speed (100 rpm) in the paste. Measuring the final set with a Vicat needle revealed to be very inaccurate for materials with slow setting (>24 h). More reliable results were obtained by considering that the set was effective when the temperature in the grout reached its maximum.

Table 5
Chemical and mineralogical composition of sulfate-resistant Portland cement

Oxides	% weight	Minerals[a]	% weight
SiO_2	19.9	C_3S	65.6
Al_2O_3	5.4	C_2S	16.0
Fe_2O_3	2.6	C_3A	4.0
CaO	65.0	C_4AF	5.6
MgO	1.4	Gypsum	4.8
K_2O	0.9	Carbonate	2.8
Na_2O	0.1		
SO_3	3.4		
S^{2-}	< 0.01		
Loss of ignition	1.0		

[a] Determined by Bogue calculation.

Table 6
Experimental design and measured responses

Run no.	H_3BO_3 (g/l)	Cl^- (g/l)	SO_4^{2-} (g/l)	PO_4^{3-} g/l)	Torque (N cm)	Final set (h)	T_{max} (°C)	R_c[a] (MPa)	Swelling[a] (μm/m)
1	0.0	1.0	0.8	44.7	5.0	15.25	65.9	41.4	919
2	17.2	1.0	0.8	34.7	8.3	21.40	61.0	38.3	1250
3	0.0	20.0	0.8	26.5	3.2	19.00	68.0	44.7	1042
4	17.2	20.0	0.8	16.6	13.5	31.00	75.7	38.1	1762
5	0.0	1.0	27.0	22.2	4.4	23.70	75.9	40.9	950
6	17.2	1.0	27.0	12.2	19.0	56.80	79.6	47.0	1366
7	0.0	20.0	27.0	4.1	9.5	15.67	86.6	64.0	1134
8	5.3	20.0	27.0	1.0	12.5	16.33	82.4	57.5	1140
9	17.2	12.8	27.0	1.0	26.4	23.33	77.9	45.8	1271
10	17.2	20.0	19.0	1.0	21.0	17.83	80.8	56.7	1316
11	8.6	1.0	0.8	39.7	8.0	23.83	63.1	38.1	852
12	0.0	10.5	0.8	35.6	4.4	19.00	67.0	41.0	810
13	0.0	1.0	13.9	33.4	5.1	16.83	73.9	43.5	767
14	17.2	10.5	0.8	25.7	22.5	24.33	67.6	43.0	1001
15	17.2	1.0	13.9	23.5	4.5	39.77	77.5	44.1	843
16	8.6	20.0	0.8	21.6	4.8	42.67	79.7	48.4	1020
17	0.0	20.0	13.9	15.3	5.0	16.50	76.7	41.4	1480
18	17.2	20	9.9	8.8	17.5	74.67	81.4	57.3	1127
19	8.6	1.0	27.0	17.2	5.2	28.00	79.5	47.6	951
20	0.0	10.5	27.0	13.1	14.3	17.20	81.4	47.2	1300
21	17.2	6.9	27.0	6.6	14.0	54.00	84.3	54.0	1153
23	11.2	16.4	27.0	1.0	13.0	24.33	80.9	63.5	934
33a	9.1	11.7	15.8	16.4	10.6	28.67	76.3	45.0	1067
33b	9.1	11.7	15.8	16.4	7.0	29.00	76.4	42.2	907
33c	9.1	11.7	15.8	16.4	4.0	27.00	78.0	46.7	822
33d	9.1	11.7	15.8	16.4	5.0	24.67	78.8	44.9	1094
33e	9.1	11.7	15.8	16.4	6.6	26.25	80.3	48.9	1224
34	4.6	6.4	8.3	30.5	5.0	19.67	74.8	47.1	790
37	13.2	15.8	8.3	16.5	4.1	68.90	72.3	48.8	1074
39	13.2	6.4	21.4	14.3	4.1	80.67	70.9	43.0	940
40	4.6	15.8	21.4	10.2	7.8	37.33	80.3	59.2	878

[a] Average values—three 4 × 4 × 16 cm specimens for each run.

4.4. Calculations

All calculations were performed with NEMROD software [38].

5. Results and discussion

Experimental data are summarized in Table 6. For each response, the model coefficients were estimated by standard least squares regression techniques (Table 7). Possible model deficiencies were looked for by using analysis of variance (ANOVA) (Table 8). Two hypotheses were tested: (H1) the lack of fit of the model is statistically not significant and (H2) the model has no explanatory effect (i.e., the regression coefficients are zero). Let $\hat{y}_i$ be the value predicted for y_i by the model, $\bar{y}$ the average of all y_i, n_e the number of replicates ($n_e = 5$), n the total number of runs ($n = 31$) and p the number of coefficients in the model ($p = 14$). The total variability in the response Y, $SST = \sum_i (y_i - \bar{y})^2$, was decomposed into two sources: the explained variability $SSR = \sum_i (\hat{y}_i - \bar{y})^2$, which was the variability in Y that could be accounted for by the model, and the unexplained variability $SSE = \sum_i (y_i - \hat{y}_i)^2$. This latter was additionally split into a sum of squares for replication error (SS_{RE}) and a sum of squares for lack of fit (SS_{LF}). The F-ratio for testing lack of fit was thus $MS_{LF}/MS_{RE} = \{SS_{LF}/[n - p - (n_e - 1)]\}/\{SS_{RE}/(n_e - 1)\}$, while

Table 7
Estimated coefficients of special cubic models in the canonical form

Variable	Coefficients			
	Torque (N cm)	T_{max} (°C)	R_c (MPa)	Expansion (μm/m)
X_1'	− 38.0	40.9	− 104.6	6952.3
X_2'	− 53.7	29.0	2.4	3450.0
X_3'	2.0	56.7	26.1	2245.6
X_4'	4.1	64.0	39.7	933.9
$X_1'X_2'$	662.4	376.9	764.7	3875.1
$X_1'X_3'$	331.9	93.6	226.5	− 3504.7
$X_2'X_3'$	127.4	178.8	219.4	− 7178.2
$X_1'X_4'$	91.1	1.4	154.5	− 5754.8
$X_2'X_4'$	85.5	68.6	73.4	− 4188.4
$X_3'X_4'$	0.5	60.7	35.1	− 2886.5
$X_1'X_2'X_3'$	− 1564.7	− 866.8	− 1535.9	− 40,944.3
$X_1'X_2'X_4'$	− 1074.7	− 422.9	− 744.7	− 25,821.2
$X_1'X_3'X_4'$	− 638.4	223.0	235.4	− 14,504.5
$X_2'X_3'X_4'$	78.0	− 113.5	− 341.1	21,032.0

Table 8
Checking for accuracy and significance of models using ANOVA

Response	Source	Sum of squares	*df*	Mean square	*F*-test	*P*-value
Torque	Regression	887.2	13	68.2	8.4	***
	Residuals	129.2	16	8.1		
	Lack of fit	103.7	12	8.6	1.4	41.4%
	Replication error	25.5	4	6.4		
	Total	1016.4	29			
T_{max}	Regression	1030.8	13	79.3	31.7	***
	Residuals	34.9	14	2.5		
	Lack of fit	23.5	10	2.4	0.8	63.3%
	Replication error	11.4	4	2.9		
	Total	1065.7	27			
R_c	Regression	877.9	13	67.5	8.3	***
	Residuals	104.7	13	8.1		
	Lack of fit	80.2	9	8.9	1.5	38.0%
	Replication error	24.5	4	6.1		
	Total	982.6	26			
Expansion	Regression	1,238,213.6	13	95247.2	5.9	***
	Residuals	241,758.0	15	16117.2		
	Lack of fit	140,522.8	11	12774.8	0.5	83.3%
	Replication error	101,235.2	4	25308.8		
	Total	1,479,971.6	28			

P-value: probability that a random variable having a *F*-distribution is greater than the *F*-test.
*** $P<.1\%$.

the *F*-ratio for testing model significance was MSR/MSE=[SSR/($p-1$)]/[SSE/($n-p$)]. A model was considered to give an adequate description of the response if hypothesis (H1) was accepted and hypothesis (H2) rejected.

A few experiments were omitted for least squares regression in order to improve the model accuracy. These runs, which were characterized by residuals (difference between experimental and calculated values) higher than twice the experimental error, were considered as erratic rather than representative of different phenomena for the following reasons:

- their number was very limited,
- they were randomly distributed in the experimental domain,
- they were different for each of the investigated responses.

5.1. Viscosity

Limited viscosity of the fresh paste corresponded to torque values <10 N cm. For higher values, stiffening was observed as soon as mixing was stopped. The special cubic model provided a good correlation of the experimental data, with the exception of one abnormal point (run no. 14), which was not taken into account in the least squares regression. From the response contour plots presented in Fig. 2, it can be seen that the phosphate concentration is a determining parameter in the control of the paste viscosity. All runs carried out with wastes the phosphate concentration of which exceeded 25 g l^{-1} led to flowing grouts. For lower phosphate concentrations, a less favorable rheology was obtained:

- in the presence of an average or strong sulfate concentration (for example, higher than 10 g l^{-1} in the absence of boron),
- in the presence of a strong chloride concentration if the boron concentration was high (for instance, $[Cl^-]>15$ g l^{-1} if [B] = 3 g l^{-1}).

The paste stiffening observed with sulfate-rich wastes is characteristic of a false set which, as previously described, results from the calcic precipitation of SO_4^{2-} into massive crystals of gypsum and/ or ettringite. Phosphate ions also

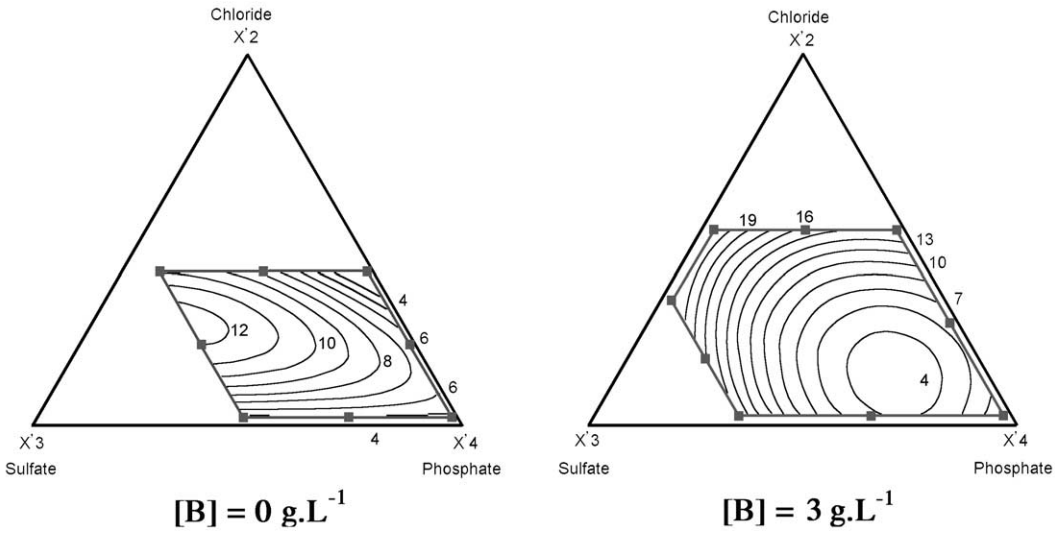

Fig. 2. Torque (N cm) contour plot in two {Cl^-, SO_4^{2-}, PO_4^{3-}} projection planes.

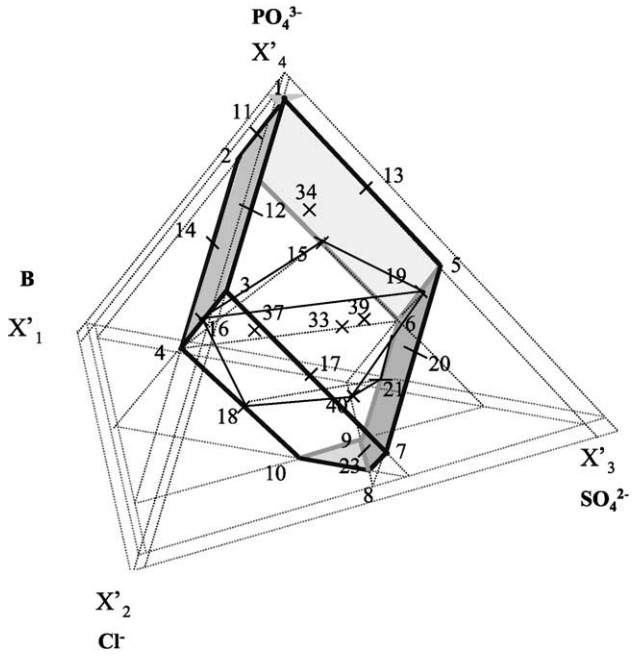

Fig. 3. Positioning within the experimental domain of concentrates leading to final set above 24 h.

precipitate in the presence of calcium. Our results show that, on the contrary to sulfate, they would rather tend to increase the fluidity of the grout under the investigated conditions, which could result from differences in the morphology of the precipitates. For example, smooth spherical particles such as fly ash are known to enhance the workability of fresh cement pastes.

5.2. Bleeding

Results concerning bleeding were very satisfactory since this phenomenon was never observed, whatever the waste composition.

5.3. Setting

Unexpected results were obtained: wastes with the highest concentrations in phosphate and borate had not the strongest retarding effect on cement hydration. The concentrates leading to materials with a final set exceeding 24 h were all located within the "center" of the experimental domain (Fig. 3) and checked both conditions:

$$[B] \geq 0.8 \text{ g l}^{-1} \text{ and } 6.6 \leq [PO_4^{3-}] \leq 23.4 \text{ g l}^{-1}$$

Given the abrupt variations of the response over the experimental domain, the special cubic polynomial presented significant lack of fit and could not be used as a prediction tool. Improved representation of the data would require either to use an alternative model (a tentative approach with a full cubic polynomial was unsuccessful) or to partition the experimental domain. In both cases, complementary experiments should be added to keep a design with good statistics.

The decrease in retardation for high contents of phosphate was also observed with simplified wastes consisting of demineralized water with increasing amounts of sodium phosphate ($[PO_4^{3-}] = 0$, 10, 30 or 50 g l^{-1}) and constant pH

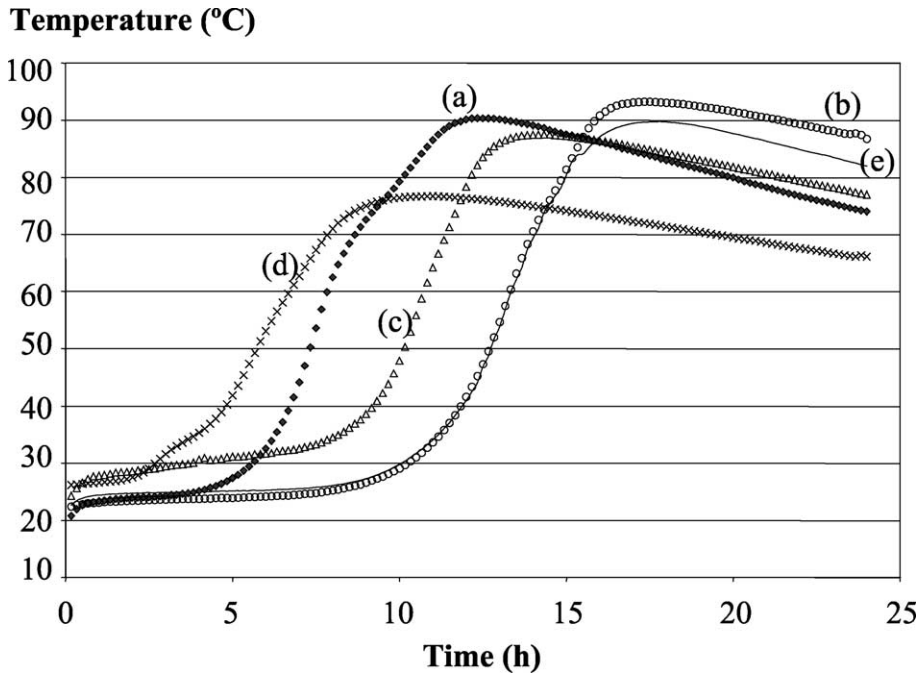

Fig. 4. Calorimetric curves relating temperature in the grout to time for simplified phosphate-containing wastes. Waste composition: pH 13.2. (a) $[PO_4^{3-}] = 0$ g· l^{-1}, $[Na^+] = 18.7$ g l^{-1}; (b) $[PO_4^{3-}] = 10$ g l^{-1}, $[Na^+] = 9.4$ g l^{-1}; (c) $[PO_4^{3-}] = 30$ g l^{-1}, $[Na^+] = 22.5$ g l^{-1}; (d) $[PO_4^{3-}] = 50$ g l^{-1}, $[Na^+] = 36.3$ g l^{-1}; (e) $[PO_4^{3-}] = 10$ g l^{-1}, $[Na^+] = 36.3$ g l^{-1}, $[NO_3^-] = 72.4$ g l^{-1}.

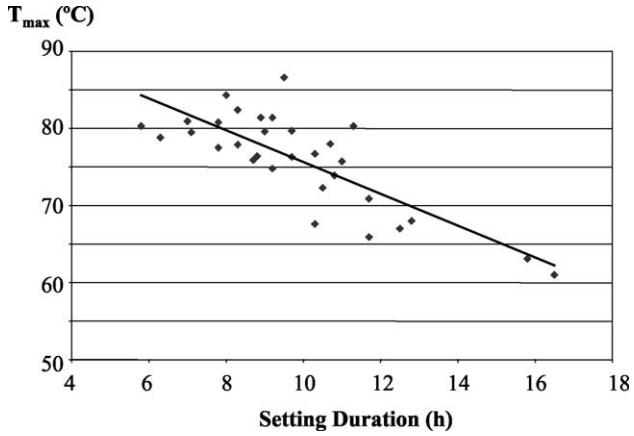

Fig. 5. Correlation between T_{max} and setting duration (initial set estimated with the Vicat needle).

(13.2), as shown in Fig. 4. Adding phosphate at low concentration (10 g l^{-1}—curve (b) of Fig. 4) caused an increase in the induction period, as compared with the probe run without phosphate (curve (a) of Fig. 4), which was consistent with the literature. However, for higher concentrations of phosphate (curves (c) and (d) of Fig. 4), the induction period shortened and, when [PO_4^{3-}] reached 50 g l^{-1}, the resulting effect was an acceleration of setting. These findings might have been due to competing actions of sodium and phosphate: at low concentrations of sodium phosphate, the retarding effect of phosphate would be preponderant, while the accelerating effect of sodium would prevail at higher concentrations. An additional run was thus carried out with a waste containing a low concentration in phosphate ([PO_4^{3-}] = 10 g l^{-1}) and a high concentration in sodium ([Na^+] = 36.3 g l^{-1}, as in the previous run with [PO_4^{3-}] = 50 g l^{-1}) due to further addition of sodium nitrate (curve (e) of Fig. 4). The heat evolution remained almost unchanged whatever the sodium concentration, which precluded the hypothesis of acceleration due to sodium. This would then indicate that phosphate behaved as a retarder at low concentration, but as an accelerator at high concentration. Similar effects, ranging from flash set to retardation of set depending on the concentration of the species, have already been reported for alkali carbonate [39] and neutral pyrophosphate [3]. For instance, sodium and potassium carbonates retarded the setting at lower dosages, but accelerated it at dosages higher than 0.1% [40]. The underlying chemistry is complex since more than one mechanism probably operates. In the case of carbonate, retardation would be caused by the formation of protective layers of calcite over the cement grains. The acceleration effect in sui table concentrations may be due to decreased permeability of the protective layer, but might also result from the removal of Ca^{2+} from the solution [39], which would enhance further dissolution of calcium ions. Moreover, direct precipitation of calcite from the solution might also be imagined, the precipitates then constituting preferential substrates for the germination and growth of hydration products, thus accelerating the hydration process. Such an explanation has been postulated to account for cement hydration acceleration in the presence of fine carbonate fillers [41]. Similar effects might occur with phosphate at high concentration. Elucidating the involved mechanisms will however require further investigation.

5.4. Heat of hydration

Adequate cement hydration of all elaborated materials was controlled by monitoring the temperature evolution within a constant mass of grout (1575 ± 1 g) placed in a Langavant semiadiabatic calorimeter after mixing. Maximum temperatures, which ranged from 61 to 86.6 °C, could be logically correlated with setting duration (Fig. 5): the shorter the setting, the higher the rate of heat liberation and the T_{max} value. The special cubic model gave a satisfactory description of the data, except for three points (runs no. 16, 21 and 39), which were omitted for the calculations.

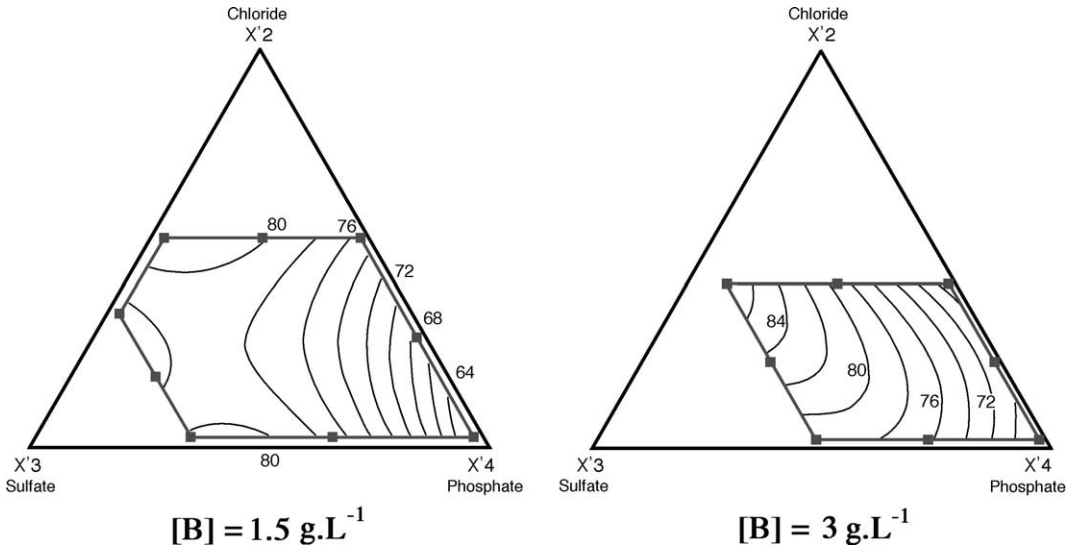

Fig. 6. T_{max} (°C) contour plot in two {Cl^-, SO_4^{2-}, PO_4^{3-}} projection planes.

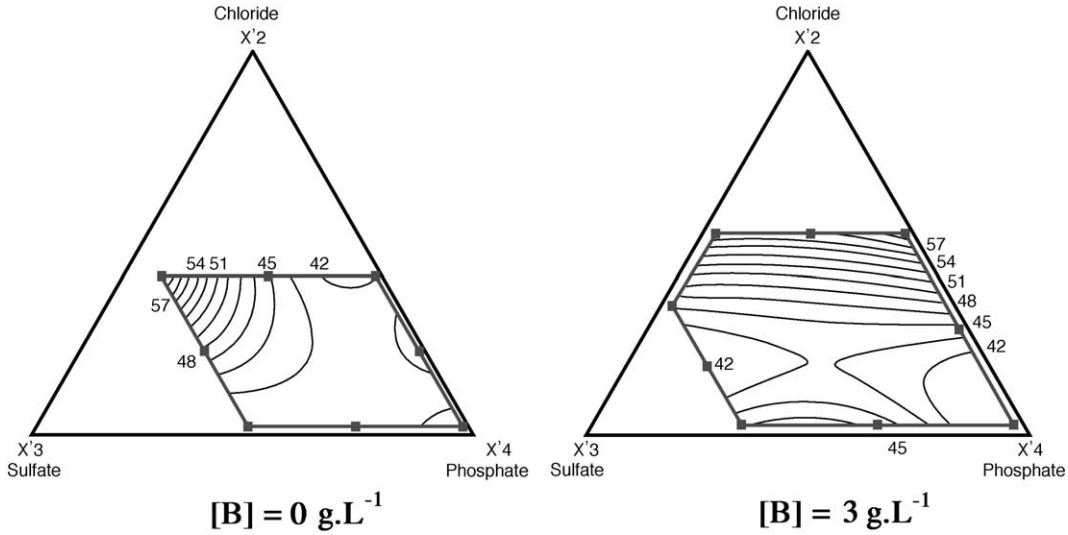

Fig. 7. Compressive strength (MPa) contour plot in two $\{Cl^-, SO_4^{2-}, PO_4^{3-}\}$ projection planes.

Response surface contour plots show that T_{max} mainly depended on the sulfate and phosphate concentrations, these two species having opposite effects (Fig. 6). A raise in T_{max} resulted from an increase in $[SO_4^{2-}]$ (especially within the range 0–15 g l^{-1}), but from a decrease in $[PO_4^{3-}]$ (especially within the range 10–50 g l^{-1}).

5.5. Compressive strength

Compressive strength measured on $4 \times 4 \times 16$ cm specimens after 90 days of curing under water at ambient temperature ranged from 38.1 to 64 MPa: the minimum required value of 8 MPa was thus largely exceeded whatever the waste composition. The special cubic model provided a good correlation of the experimental data (with the exception of run no. 4, 21, 23 and 40 as shown by residual analysis) and was regarded as an acceptable predictor. Response surface plots are presented in Fig. 7. For a low concentration of boron ($[B] < 1.5$ g l^{-1}), the major effect was a decrease in compressive strength of the solidified wastes when the phosphate concentration increased. For higher concentrations of boron ($[B] \approx 3$ g l^{-1}), the chloride concentration turned to be the most influencing parameter: increasing $[Cl^-]$ within the range 10–20 g l^{-1} caused a significant increase in strength. Chloride has been long known to accelerate both setting and hardening of Portland cement concrete, the effect on strength decreasing however with time. This could explain why, after 90 days of curing, the chloride action on strength was only detectable for wastes with high contents of cement hydration retarder.

5.6. Expansion during curing under water

Solidified waste forms expanded during wet curing. Expansion, which was associated with significant water penetration through diffusion and capillary suction, was

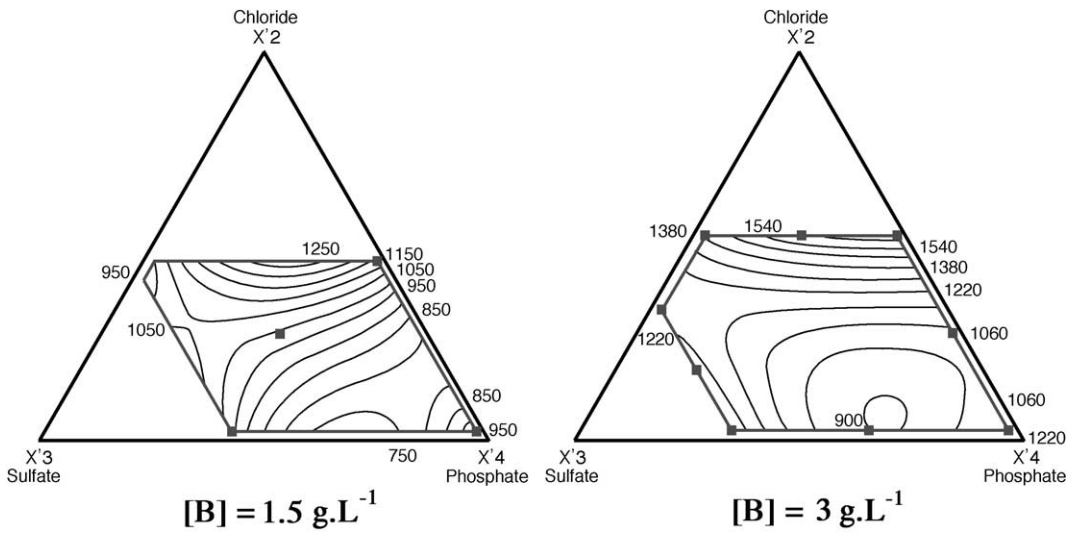

Fig. 8. Expansion (μm/m) contour plot in two $\{Cl^-, SO_4^{2-}, PO_4^{3-}\}$ projection planes.

rapid during the first month, and subsequently slowed down. After 90 days, swelling ranged from 740 to 1762 μm/m depending on the waste composition, but didn't cause any macroscopic damage of the samples. With the exception of runs no. 18 and 40, the special cubic model provided very good fit of the data and was used as a prediction tool. Response surface contour plots show that expansion was decreased by increasing the phosphate concentration in the waste (Fig. 8). On the contrary, high contents of chloride or sulfate had a negative effect, especially if combined with high concentrations of boron, since they induced significant swelling of the $4 \times 4 \times 16$ cm specimens. Marked expansion and cracking due to gypsum and/ or ettringite formation might have been expected for solidified waste forms with the highest concentrations in sulfate. However, after 90 days of curing, the effect of sulfate was not outstanding, as compared with the other factors (additional characterizations are under way to confirm this trend on a larger time scale). This might have resulted from the low C_3A content in the cement used, which improved its resistance to sulfate attack. SEM observations of fracture and polished surfaces of the samples with high contents of chloride and/or sulfate revealed the absence of destructive calcium oxychloride, ettringite or U phase. In a similar way, the presence of platey hexagonal crystals of AFm phases couldn't be detected. Nevertheless, in microporous regions of the samples, X-ray microanalysis showed calcium and silicon to be associated with aluminium, sulfur and chloride, which could indicate the existence of poorly crystalline calcium monosulfoaluminate, chloroaluminate or chlorosulfoaluminate intimately mixed with C–S–H.

6. Conclusion

The main properties of the investigated formulation, as regards process and final disposal requirements, are summarized in Table 9. The presence of phosphate at high concentration (>25 g l^{-1}) in the waste appeared to be very favorable since most features of the resulting material were improved: setting time, rate of heat production during cement hydration and swelling during wet curing were decreased, while workability of the grout was enhanced. The correlative decrease in compressive strength remained acceptable, the minimum required value still being largely exceeded. These unexpected effects of phosphate will be the subject of an academic study on a simplified reactive medium.

From a more general point of view, the experimental design methodology used in this study proved to be very fruitful given the complexity of the system under investigation. In contrast to the classical one-variable-at-a-time approach, the values of all the factors were varied simultaneously in each experiment. The way in which they were varied was however programmed and rational. While this could appear somewhat disturbing at first sight, this approach offered several advantages: the trials were kept to a reasonable number, interactions between factors could be detected, results were obtained with a good precision, and operational models were built from the data. This methodology being general, it could be used in other types of cement formulation studies for waste management.

Table 9
Main properties of the investigated formulation

• Occurrence of setting whatever the waste composition	• Absence of bleeding
• Final set always above 5 h and exceeding 24 h for wastes ith boron ([B]>0.8 g l^{-1}) and phosphate at medium concentration ($6 < [PO_4^{3-}] < 24$ g l^{-1})	• Rapid heat production (T_{max}>80 °C) during cement hydration for wastes with low content of phosphate (<10 g l^{-1}) and medium or high content of sulfate (>15 g l^{-1})
• Stiffening of the grout for wastes with low or medium content of phosphate ($[PO_4^{3-}] < 25$ g l^{-1}) and medium or high concentration of sulfate (>10 g l^{-1}) or high concentration of borate and chloride ([B] ≈ 3 g l^{-1}, $[Cl^-]$>15 g l^{-1})	• High compressive strength of solidified waste forms after 90 days of wet curing at 20 °C • No cracking of solidified waste forms after 90 days of wet curing at 20 °C

Acknowledgements

A. Vernier, M. Rodriguez, T. Ravel and P. Chenavas are deeply acknowledged for their contribution to the experimental work.

References

[1] Improved cement solidification of low and intermediate level radioactive waste, AIEA Technical Report Series No. 350, 1993.
[2] G.E.P. Box, K.B. Wilson, On the experimental attainment of optimum conditions, J. R. Stat. Soc., Ser. B 30 (1968) 349–358.
[3] W. Lieber, Effect on inorganic admixtures on the setting and hardening of Portland cement, Zem.-Kalk-Gips 2 (1973) 75–79.
[4] A. Joisel, Admixtures for Cement (Published by the author), Ecole Polytechnique, Paris, 1973.
[5] A. Demribas, S. Karshloglu, The effect of boric acid sludges containing borogypsum on properties of cement, Cem. Concr. Res. 25 (1995) 1381–1384.
[6] S. Hernandez, A. Guerrero, S. Goni, Leaching of borate waste cement matrices: pore solution and solid phase characterization, Adv. Cem. Res. 12 (2000) 1–8.
[7] J. Bensted, I.C. Callaghan, A. Lepre, Comparative study of the efficiency of various borate compounds as set retarders of Class G oilwell cement, Cem. Concr. Res. 21 (1991) 663–668.
[8] L. Ben-Dor, Y. Rubinsztain, The influence of phosphate on the hydration of cement minerals studied by DTA and TG, Thermochim. Acta 30 (1979) 9–14.
[9] L.J. Csenteyi, F.P. Glasser, Borate retardation of cement set and phase relations in the system $Na_2O–CaO–B_2O_3–H_2O$, Adv. Cem. Res. 7 (25) (1995) 13–19.
[10] C. Roux, Conditioning of radioactive concentrates with high boron content, formulation and characterization, Thèse de l'Université Paris Sud, France, 1989.

[11] H. Akhter, F.K. Cartledge, A. Roy, M.E. Tittlebaum, A study of the effect of nickel chloride and calcium chloride on hydration of Portland cement, Cem. Concr. Res. 23 (1993) 833–842.
[12] P.W. Brown, C.L. Harner, E.J. Prosen, The effect of inorganic salts on tricalcium silicate hydration, Cem. Concr. Res. 16 (1986) 17–22.
[13] C.R. Cheeseman, S. Asavapisit, Effect of calcium chloride on the hydration and leaching of lead-retarded cement, Cem. Concr. Res. 29 (1999) 885–892.
[14] V.S. Ramachandran, Possible states of chloride in the hydration of tricalcium silicate in the presence of calcium chloride, Mater. Constr. 4 (1971) 3–12.
[15] G. Blunk, On the distribution of chloride between the hardening cement paste and its pore solution, Proc. 8th Int. Congr. Chem. FINEP 4 (1986) 85–90 (Rio de Janeiro).
[16] H.G. Midgley, J.M. Ilston, The penetration of chlorides into hardened cement pastes, Cem. Concr. Res. 14 (1984) 546–558.
[17] U.A. Birnin-Yauri, F.P. Glasser, Friedel's salt $Ca_2{\cdot}Al(OH)_6(Cl,OH){\cdot}2H_2O$; its solid solutions and their role in chloride binding, Cem. Concr. Res. 28 (12) (1998) 1713–1723.
[18] A.K. Suryavanshi, J.D. Scantlebury, S.B. Lyon, Mechanism of Friedel's salt formation in cements rich in tri-calcium aluminate, Cem. Concr. Res. 26 (5) (1996) 717–727.
[19] F.P. Glasser, K. Luke, M.J. Angus, Modification of cement pore fluid compositions by pozzolanic additives, Cem. Concr. Res. 18 (1988) 165–178.
[20] A.K. Suryavanshi, J.D. Scantlebury, S.B. Lyon, The binding of chloride ions by sulphate resistant Portland cement, Cem. Concr. Res. 25 (1995) 581–592.
[21] O. Mejhlede Jensen, M.S.H. Korzen, H.J. Jakobsen, J. Skibsted, Influence of cement constitution and temperature on chloride binding in cement paste, Adv. Cem. Res. 12 (2) (2000) 57–64.
[22] J. Tritthart, Chloride binding in cement, the influence of the hydroxide concentration in the pore solution of hardened cement on chloride binding, Cem. Concr. Res. 19 (1989) 683–691.
[23] Y. Xu, The influence of sulphates on chloride binding and pore solution chemistry, Cem. Concr. Res. 27 (12) (1997) 1841–1850.
[24] H.F.W. Taylor, Cement Chemistry, Thomas Telford Publishing, London, 1997.
[25] Y. Fu, J. Ding, J.J. Beaudoin, Expansion of Portland cement mortar due to internal sulfate attack, Cem. Concr. Res. 27 (9) (1997) 1299–1306.
[26] R. Yang, C.D. Lawrence, J.H. Sharp, Delayed ettringite formation in 4-year old cement pastes, Cem. Concr. Res. 26 (11) (1996) 1649–1659.
[27] R. Yang, C.D. Lawrence, C.J. Linsdale, J.H. Sharp, Delayed ettringite formation in heat-cured Portland cement mortars, Cem. Concr. Res. 29 (1999) 17–25.
[28] I. Odler, J. Colan Subauste, Investigation on cement expansion associated with ettringite formation, Cem. Concr. Res. 29 (1999) 731–735.
[29] R.S. Gollop, H.F.W. Taylor, Microstructural and microanalytical studies of sulfate attack: IV. Reactions of a slag cement paste with sodium and magnesium sulfate solutions, Cem. Concr. Res. 26 (7) (1996) 1013–1028.
[30] R.S. Gollop, H.F.W. Taylor, Microstructural and microanalytical studies of sulfate attack: III. Sulfate-resisting Portland cement: reactions with sodium and magnesium sulfate solutions, Cem. Concr. Res. 25 (7) (1995) 1581–1590.
[31] G. Li, P. Le Bescop, M. Moranville, Expansion mechanism associated with the secondary formation of the U phase in cement-based systems containing high amounts of Na_2SO_4, Cem. Concr. Res. 26 (2) (1996) 195–201.
[32] H. Scheffé, Experiments with mixtures, J. R. Stat. Soc., Ser. B 20 (1958) 344–360.
[33] R.D. Snee, Design and analysis of mixture experiments, J. Qual. Technol. 3 (4) (1971) 159–169.
[34] R.P. Crosier, Mixture experiments: geometry and pseudocomponents, Technometrics 26 (1984) 209–216.
[35] H. Scheffé, The simplex-centroid design for experiments with mixtures, J. R. Stat. Soc., Ser. B 25 (1965) 235–263.
[36] R.A. Mac Lean, V.L. Anderson, Extreme vertices design of mixture experiments, Technometrics 8 (1966) 447–454.
[37] T.J. Mitchell, An algorithm for the construction of D-optimal experimental designs, Technometrics 16 (1974) 203–210.
[38] D. Mathieu, J. Nony, R. Phan Tan Luu, NEMROD-W version 99-01, LPRAI, Marseille, France.
[39] H. Ushiyama, Y. Kawano, N. Kamegai, 8th ICCC 3 (1986) 154.
[40] G.L. Valenti, V. Sabatelli, The influence of alkali carbonates on the setting and hardening of Portland and pozzolanic cements, Silic. Ind. 45 (1980) 237–242.
[41] M. Nehdi, Why some carbonate fillers cause rapid increase of viscosity in dispersed cement-based materials, Cem. Concr. Res. 30 (2000) 1663–1669.